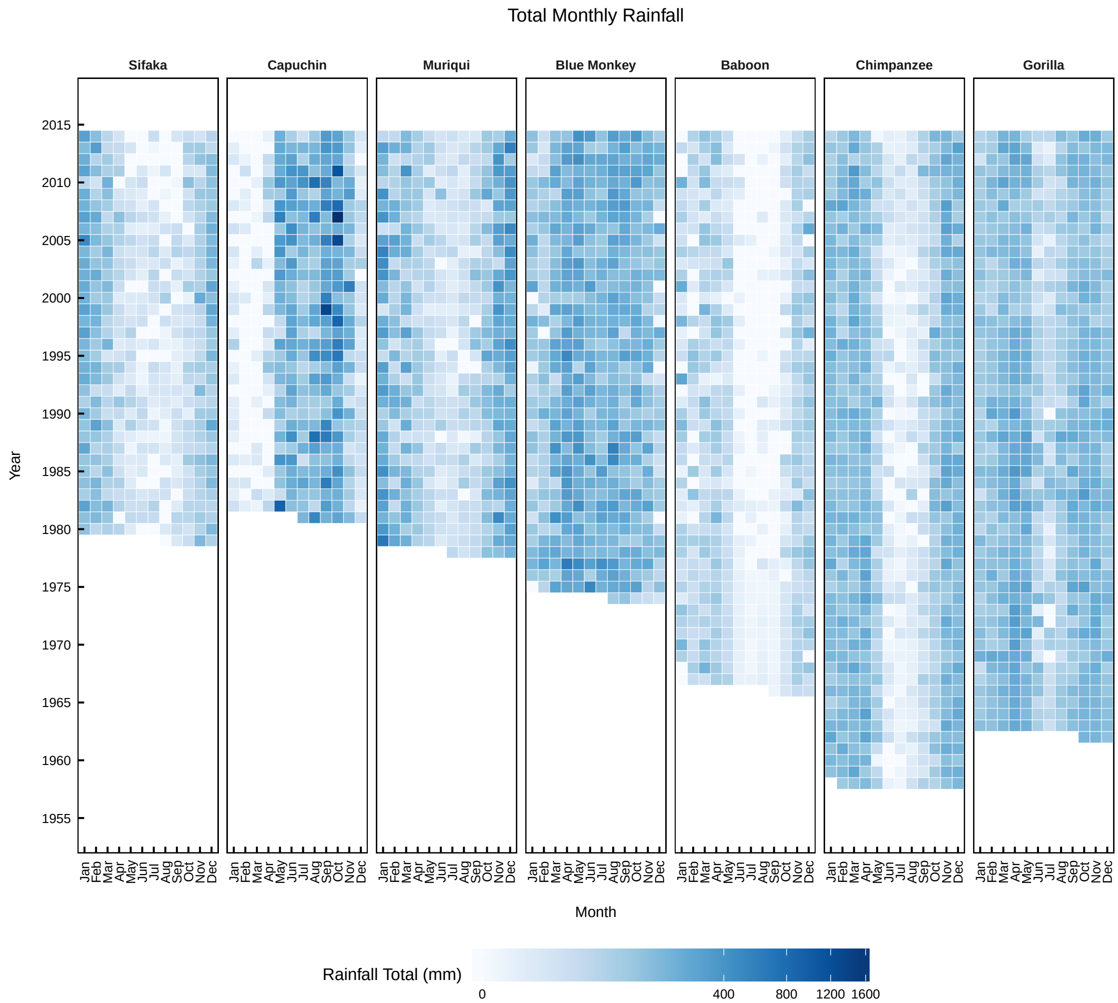

Fig. S1: Monthly rainfall totals for the seven study sites from several different data sources (see Fig. S2).

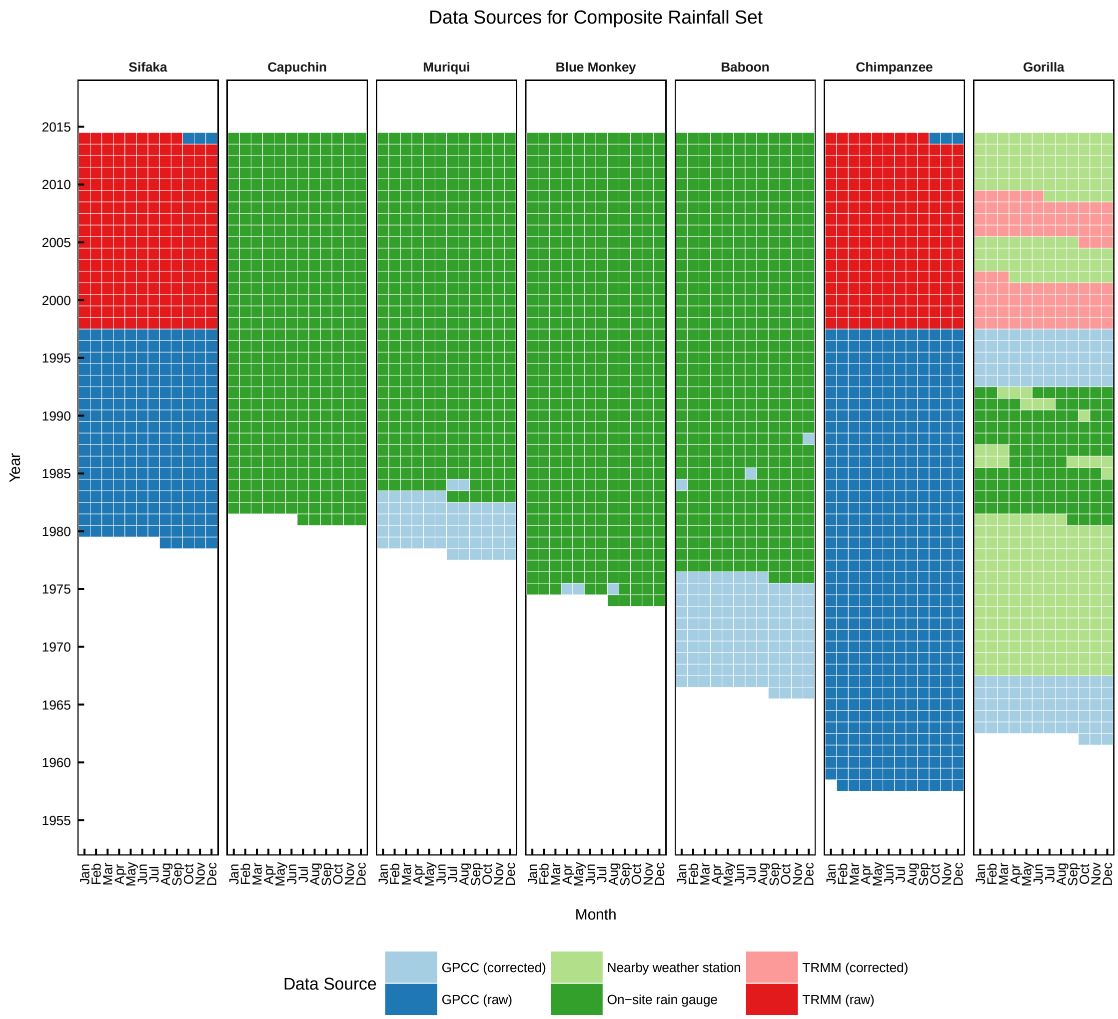

Fig. S2: Data sources for the monthly rainfall values shown in Fig. S1.

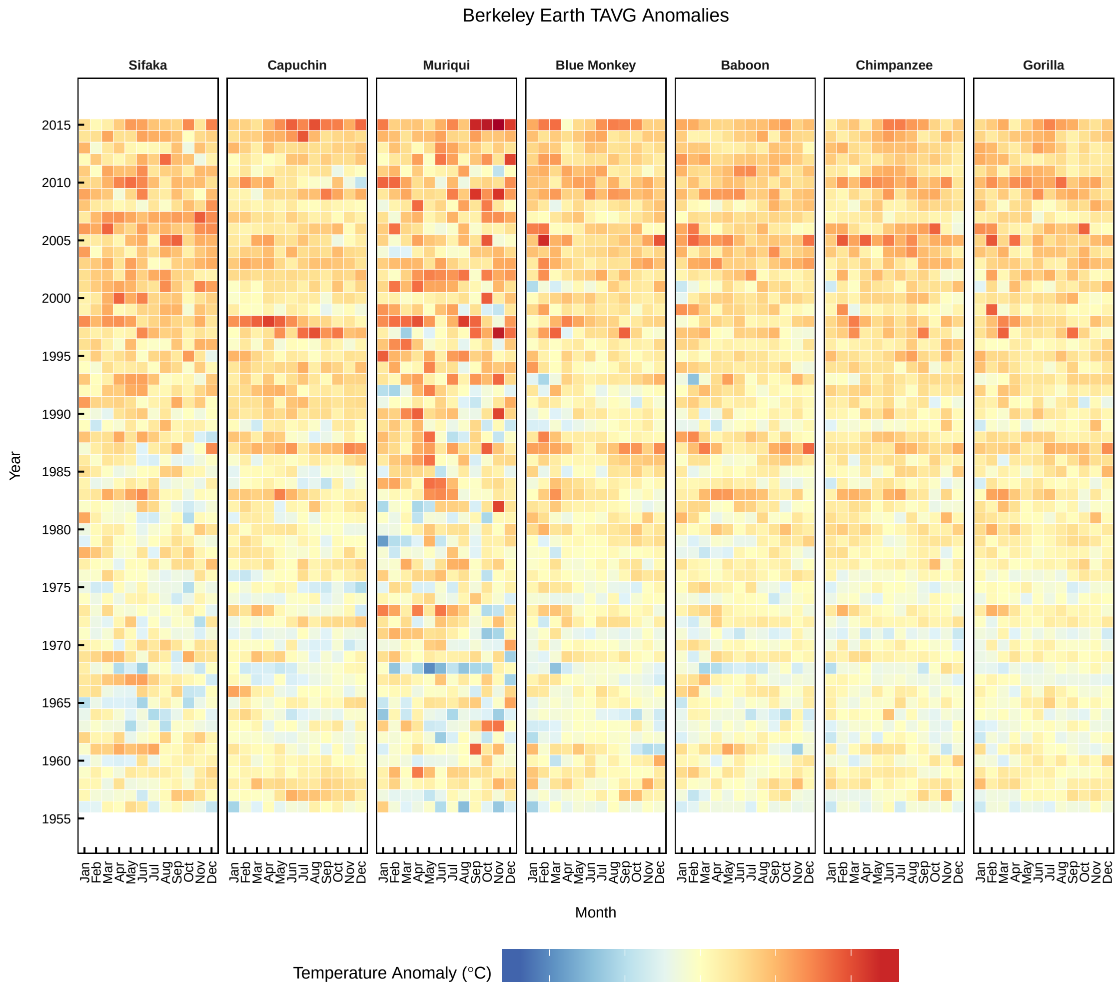

Fig. S3: Monthly average temperature anomalies for the seven study sites. Data from Berkeley Earth.

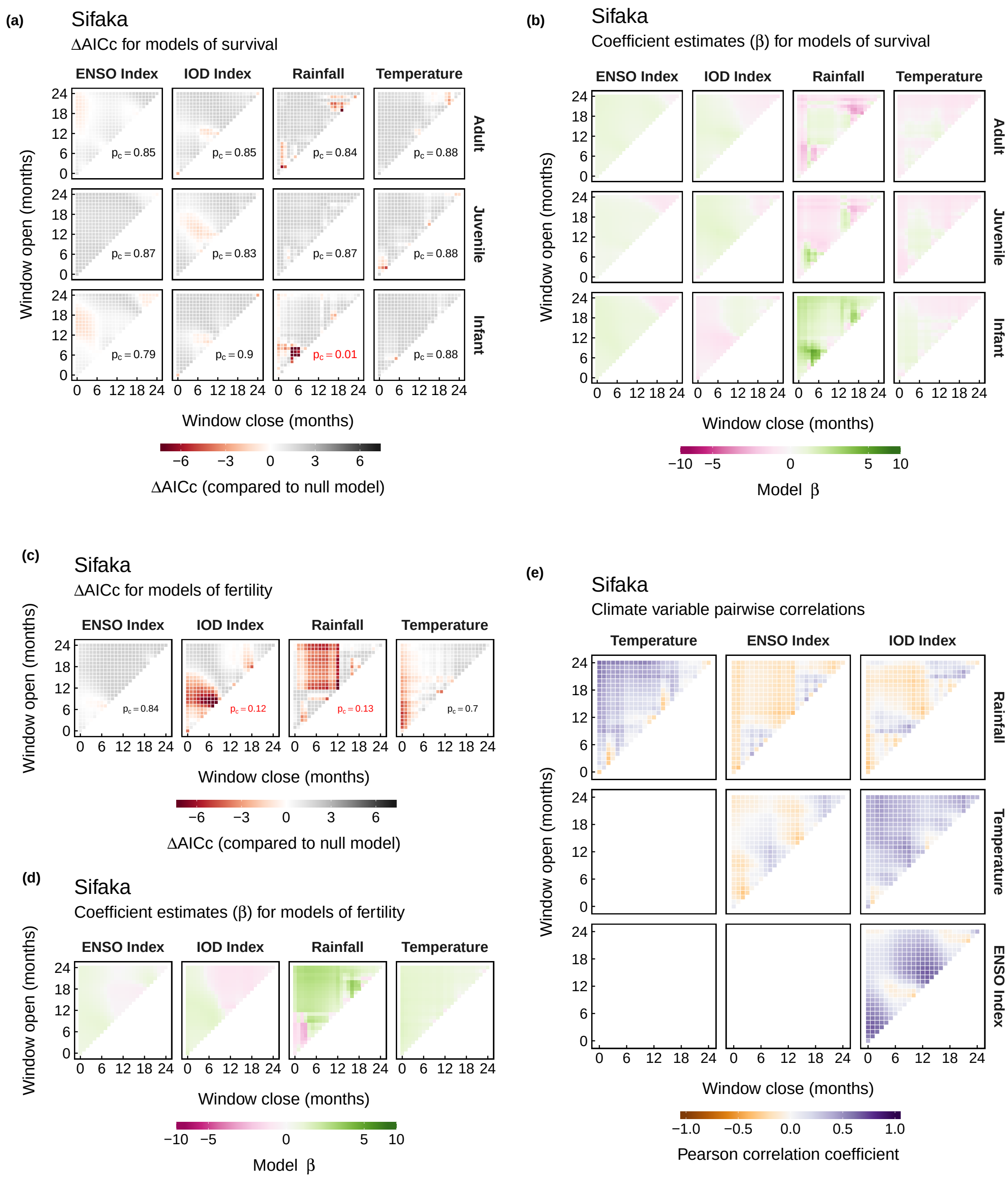

Fig. S4: ΔAICc values for climate models of Verreaux's sifaka adult, juvenile, and infant survival rates **(a)** and adult female fertility rates **(c)** for each climatic time window. The components of the plot are as described in Fig. 3a. Coefficient estimates for the climate variable term for survival models **(b)** and fertility models **(d)** in each time window. **(e)** Within-site pairwise correlations between climate variables for time window for the Verreaux's sifaka study site.

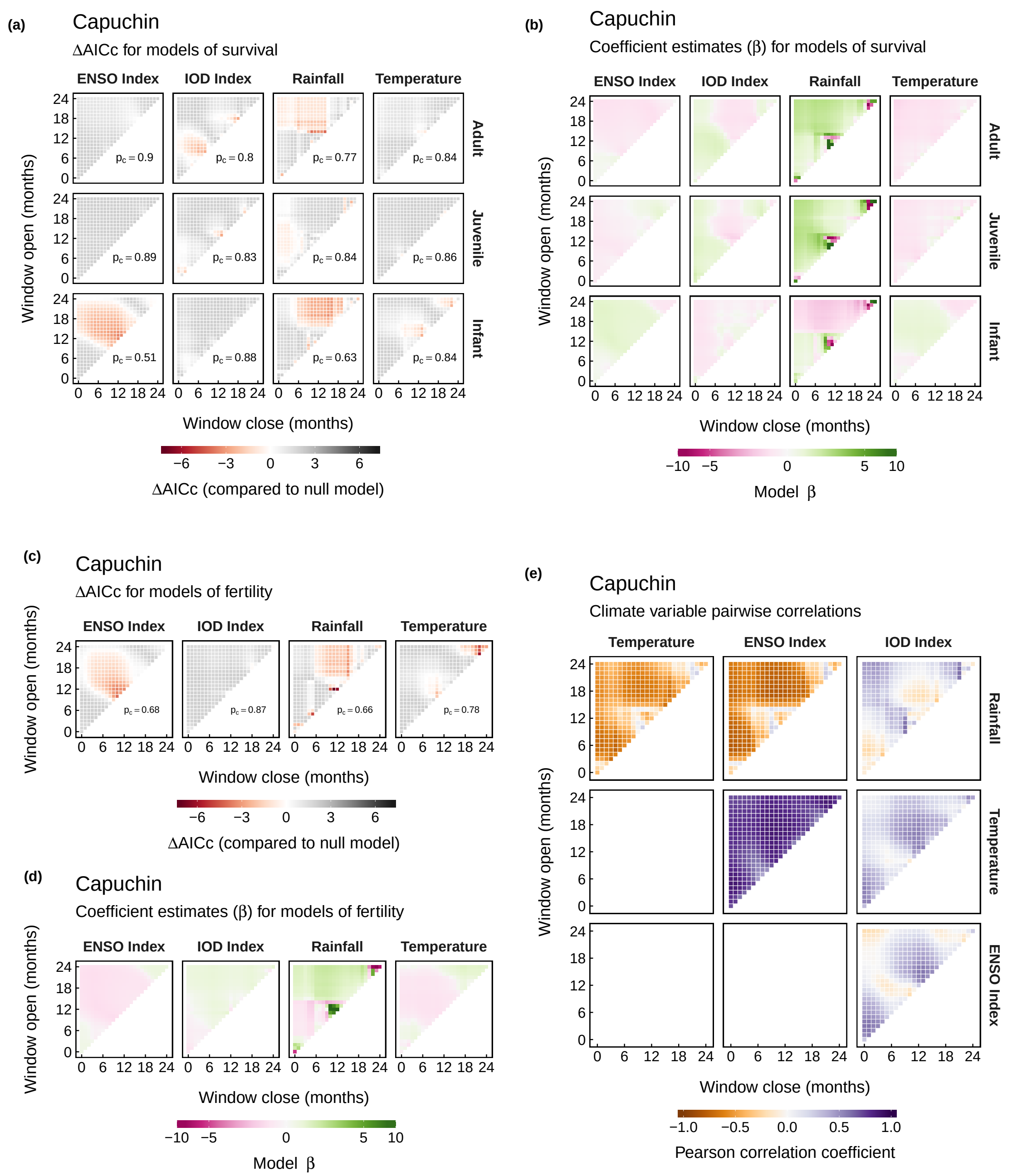

Fig. S5: ΔAICc values for climate models of white-faced capuchin adult, juvenile, and infant survival rates **(a)** and adult female fertility rates **(c)** for each climatic time window. The components of the plot are as described in Fig. 3a. Coefficient estimates for the climate variable term for survival models **(b)** and fertility models **(d)** in each time window. **(e)** Within-site pairwise correlations between climate variables for time window for the white-faced capuchin study site.

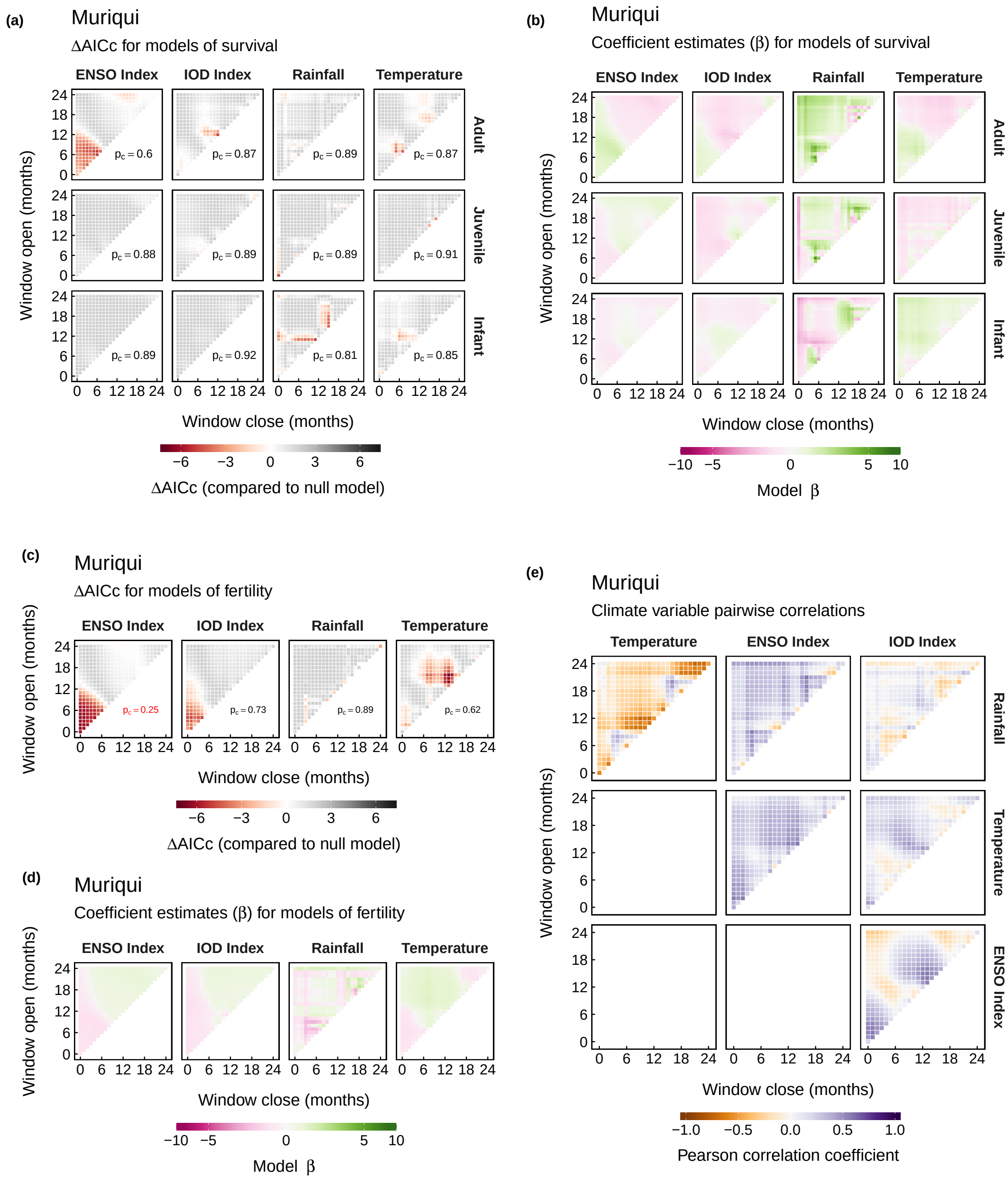

Fig. S6: ΔAICc values for climate models of northern muriqui adult, juvenile, and infant survival rates **(a)** and adult female fertility rates **(c)** for each climatic time window. The components of the plot are as described in Fig. 3a. Coefficient estimates for the climate variable term for survival models **(b)** and fertility models **(d)** in each time window. **(e)** Within-site pairwise correlations between climate variables for time window for the northern muriqui study site.

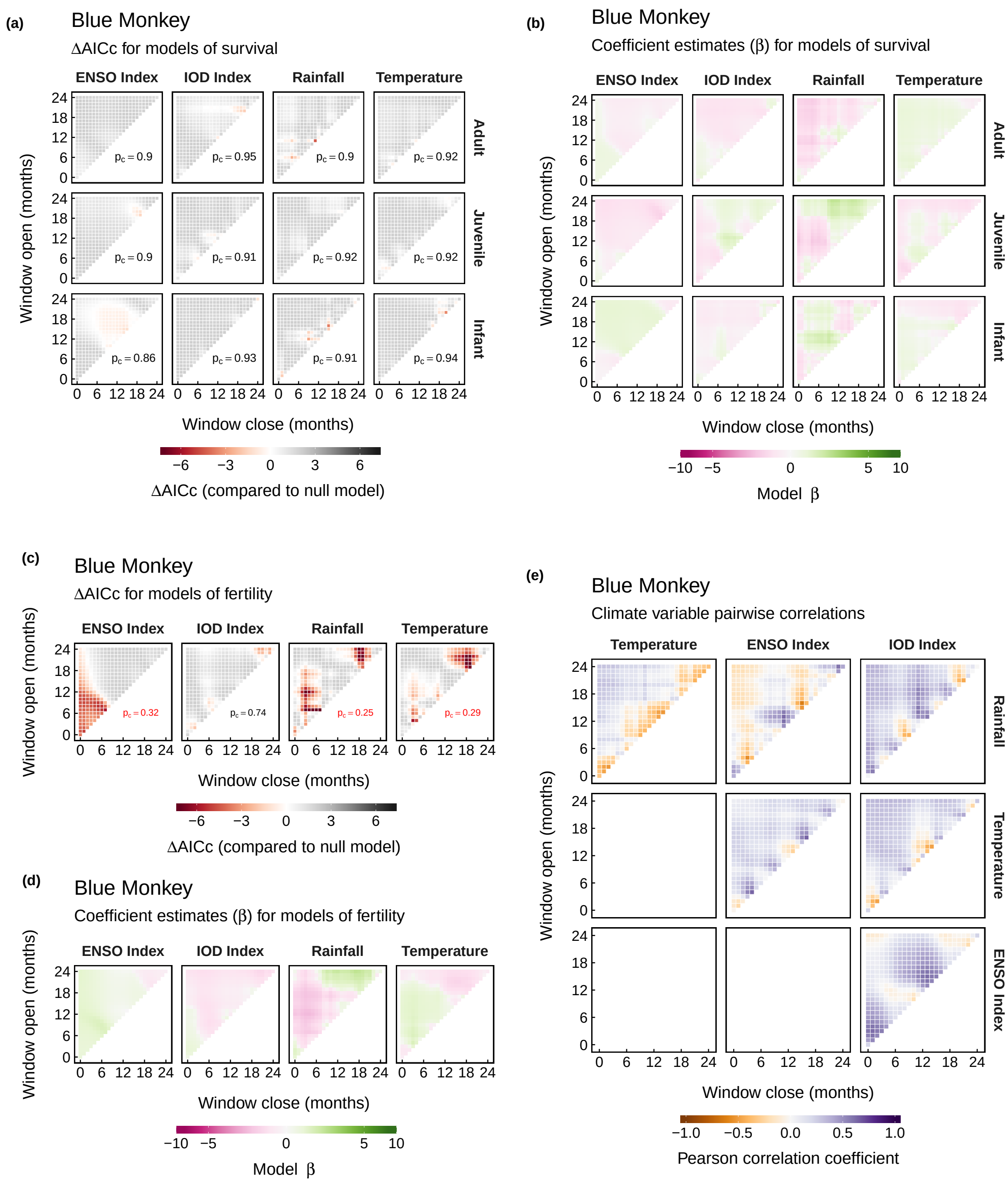

Fig. S7: ΔAICc values for climate models of blue monkey adult, juvenile, and infant survival rates **(a)** and adult female fertility rates **(c)** for each climatic time window. The components of the plot are as described in Fig. 3a. Coefficient estimates for the climate variable term for survival models **(b)** and fertility models **(d)** in each time window. **(e)** Within-site pairwise correlations between climate variables for time window for the blue monkey study site.

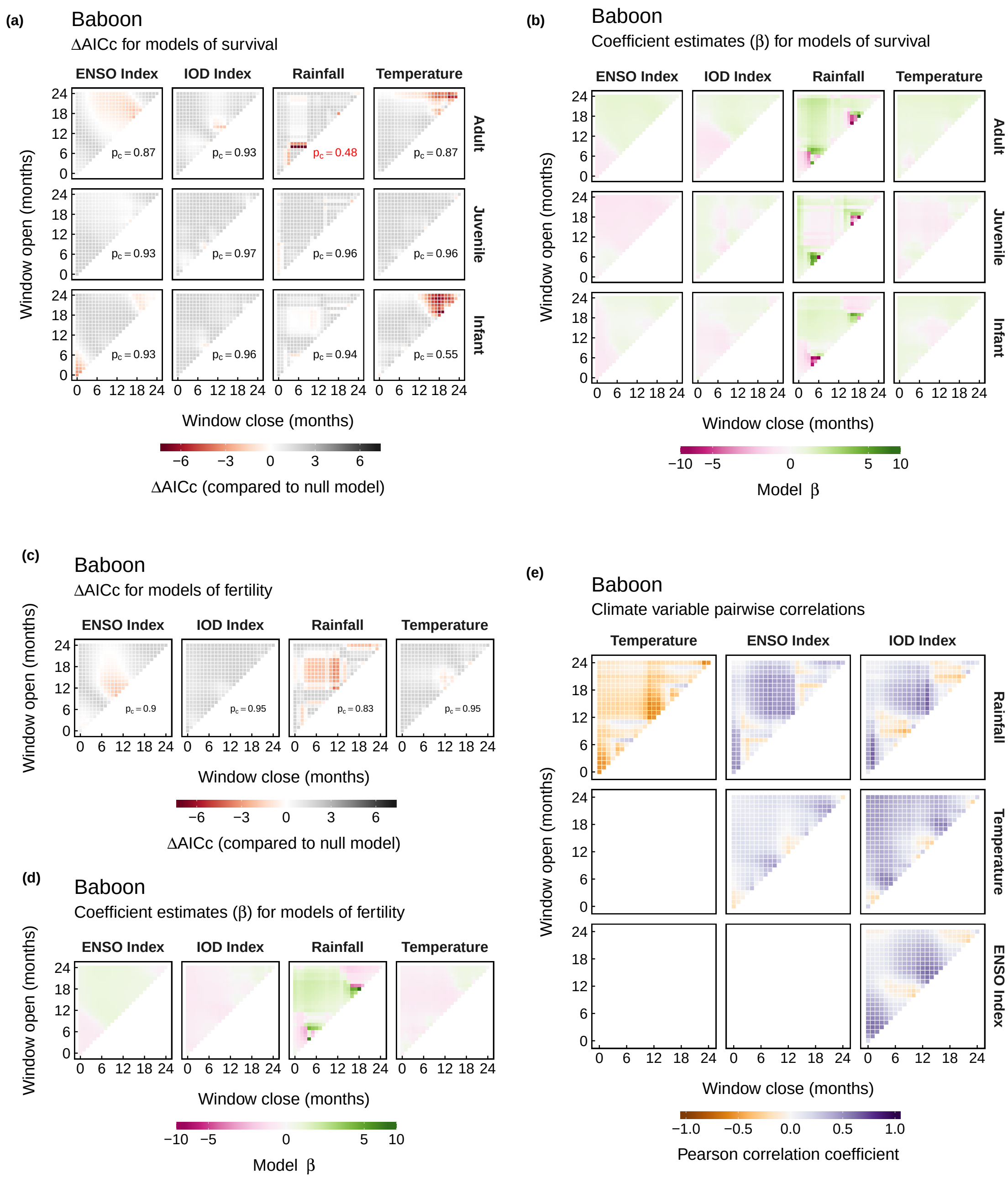

Fig. S8: ΔAICc values for climate models of yellow baboon adult, juvenile, and infant survival rates **(a)** and adult female fertility rates **(c)** for each climatic time window. The components of the plot are as described in Fig. 3a. Coefficient estimates for the variable term for survival models **(b)** and fertility models **(d)** in each time window. **(e)** Within-site pairwise correlations between climate variables for time window for the yellow baboon study site.

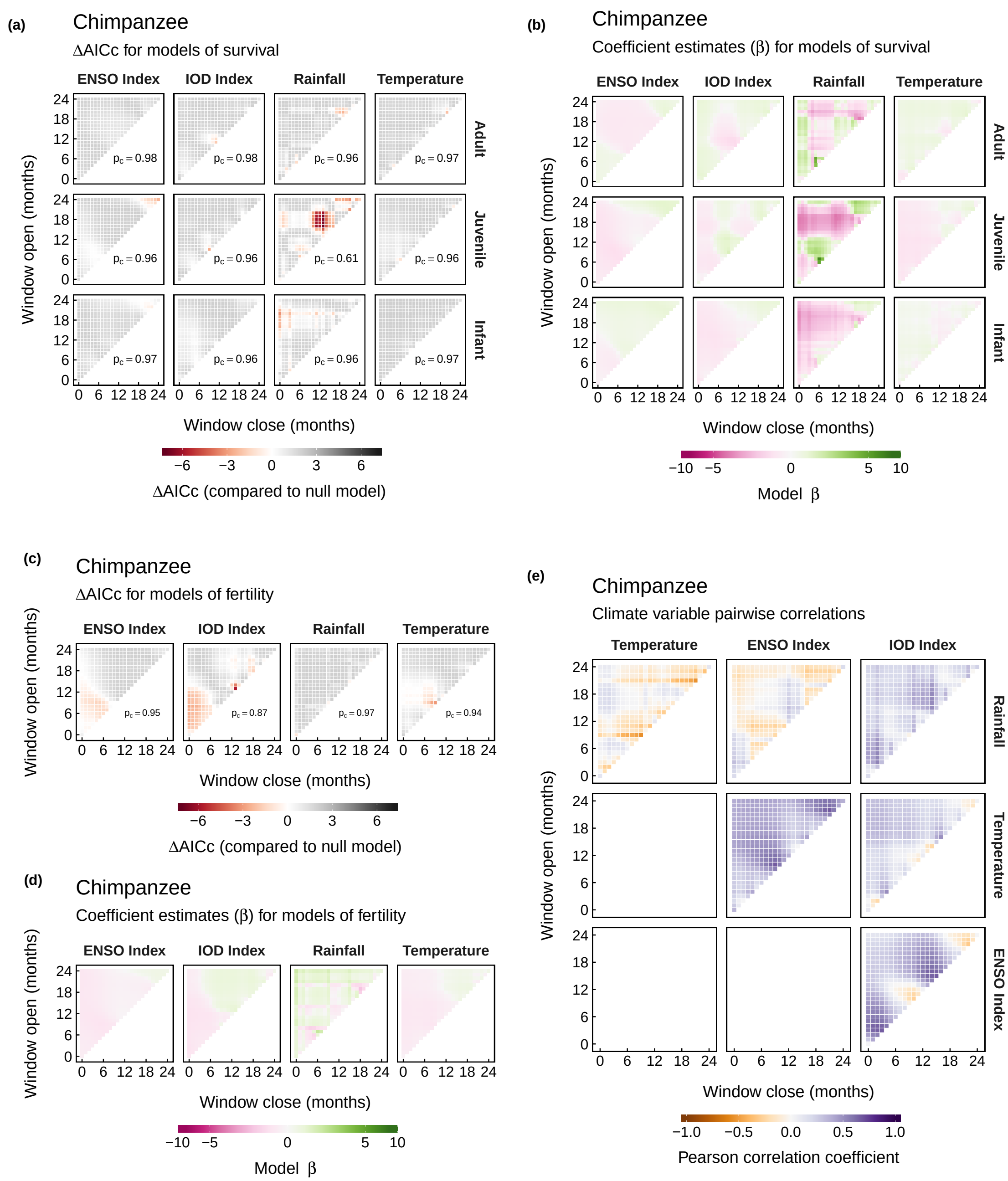

Fig. S9: ΔAICc values for climate models of eastern chimpanzee adult, juvenile, and infant survival rates **(a)** and adult female fertility rates **(c)** for each climatic time window. The components of the plot are as described in Fig. 3a. Coefficient estimates for the climate variable term for survival models **(b)** and fertility models **(d)** in each time window. **(e)** Within-site pairwise correlations between climate variables for time window for the eastern chimpanzee study site.

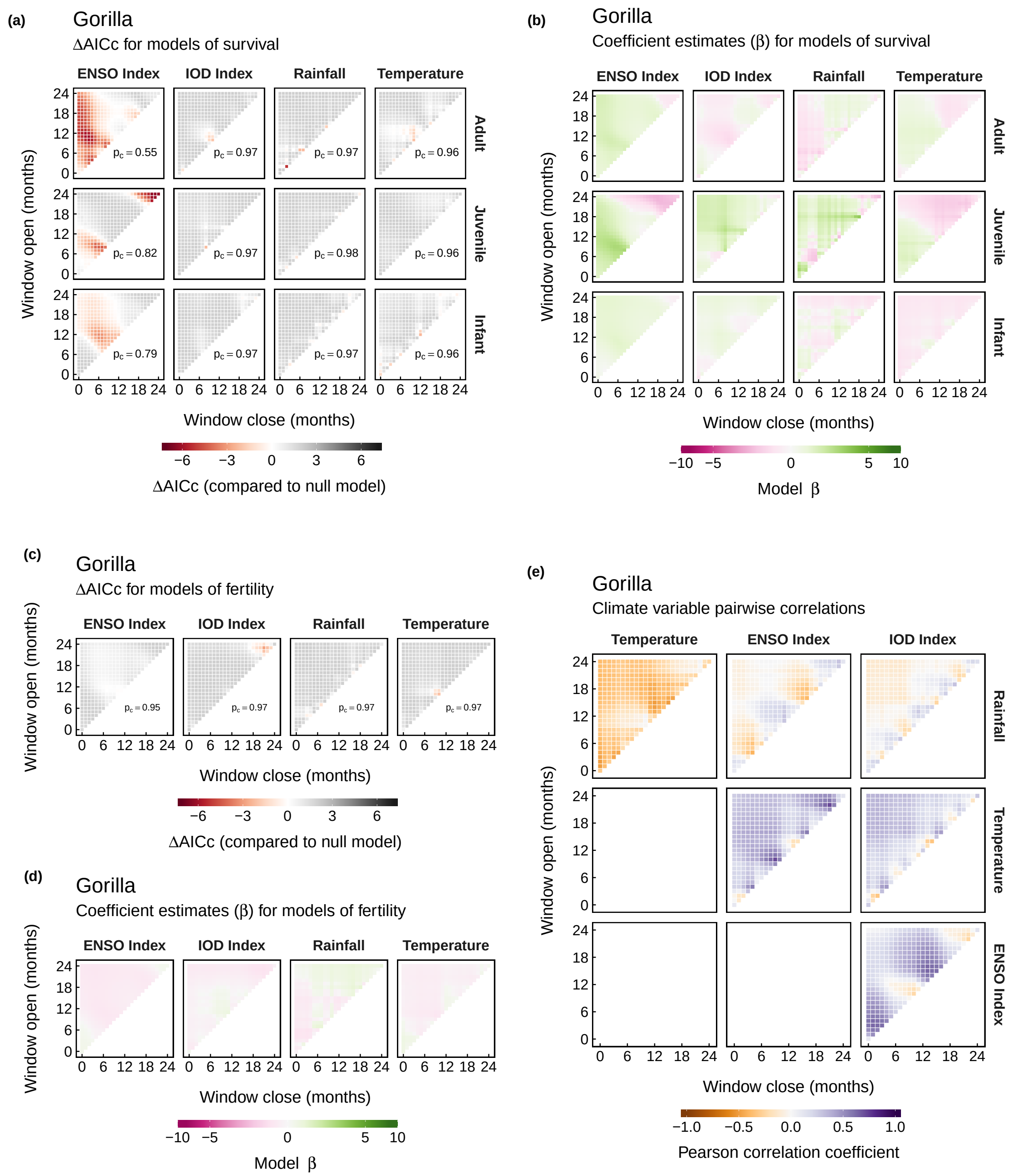

Fig. S10: ΔAICc values for climate models of mountain gorilla adult, juvenile, and infant survival rates **(a)** and adult female fertility rates **(c)** for each climatic time window. The components of the plot are as described in Fig. 3a. Coefficient estimates for the climate variable term for survival models **(b)** and fertility models **(d)** in each time window. **(e)** Within-site pairwise correlations between climate variables for time window for the mountain gorilla study site.

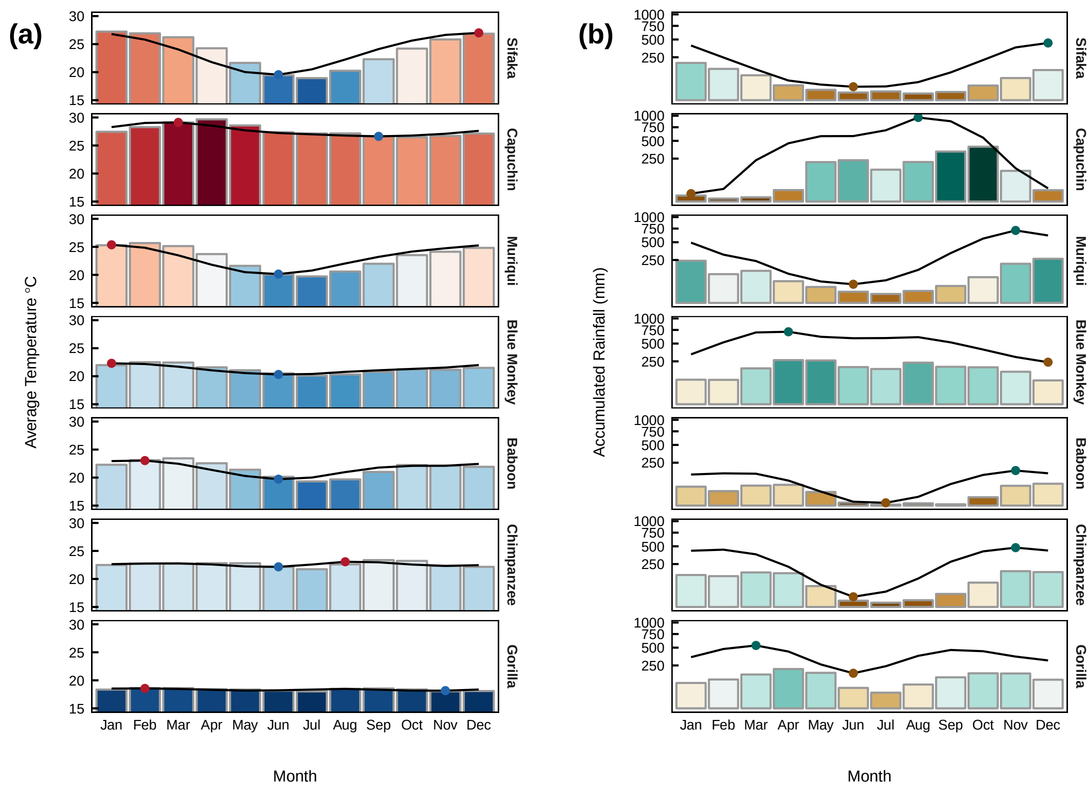

Fig. S11: Determination of extreme quarters (i.e., three consecutive months) at each study site. **(a)** Warmest and coldest quarters. The colored bars show long-term monthly means values of average temperature. The black lines show the mean of the focal month and the two months that follow. Red dots indicate the start month of the warmest quarter and blue dots indicate the start month of the coldest quarter for each site. **(b)** Wettest and driest quarters. The colored bars show long-term monthly means values of accumulated rainfall. The black lines show the sum of the focal month and the two months that follow. Blue dots indicate the start month of the wettest quarter and brown dots indicate the start month of the driest quarter for each site.

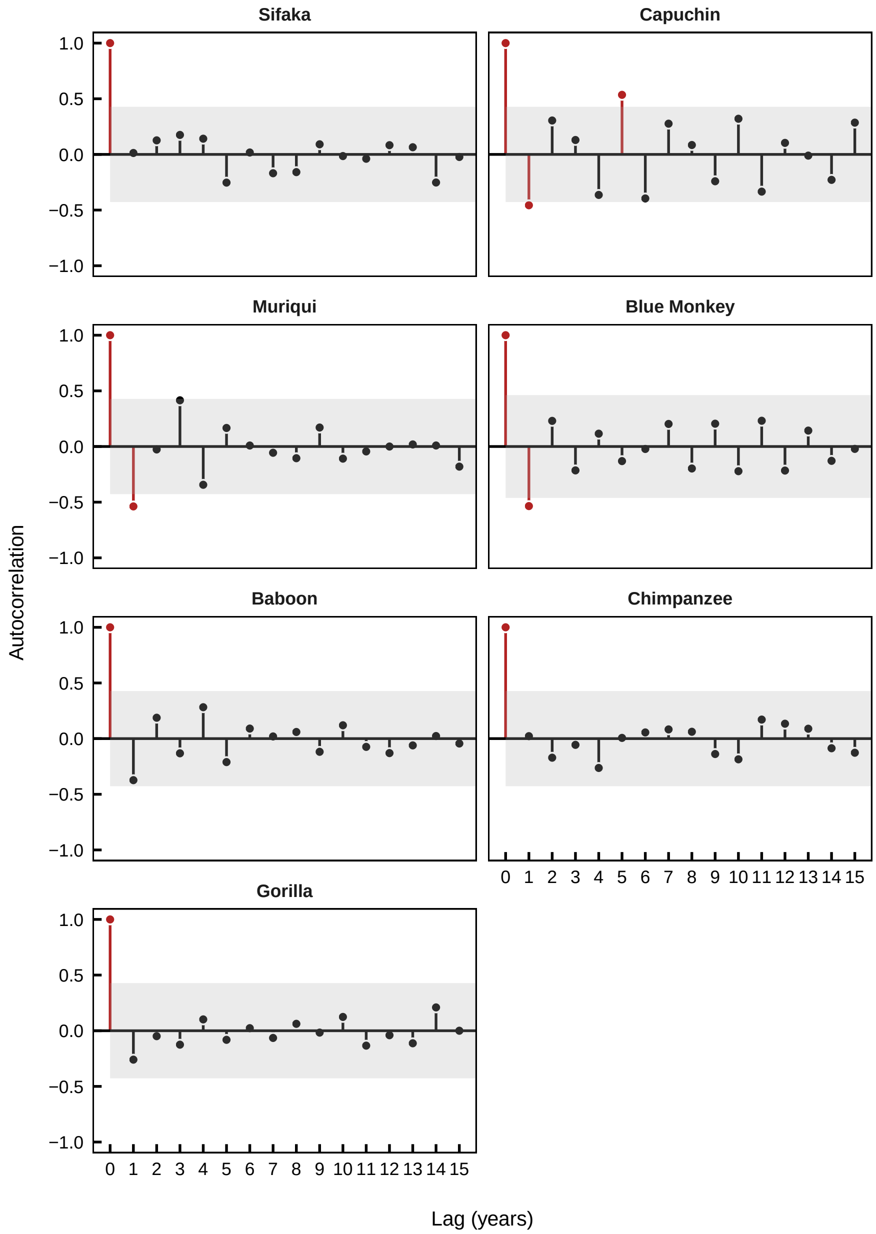

Fig. S12: Autocorrelation in population-level annual fertility rates for lags up to 15 years. The gray region shows a 95% confidence interval for the autocorrelation function; autocorrelations falling outside this region (highlighted in red) are significantly different from zero. Significant negative 1-year-lagged autocorrelations are evident in capuchins, muriquis, and blue monkeys. This indicates a pattern in which years with large infant cohorts tend to be followed by years with smaller infant cohorts and vice versa.

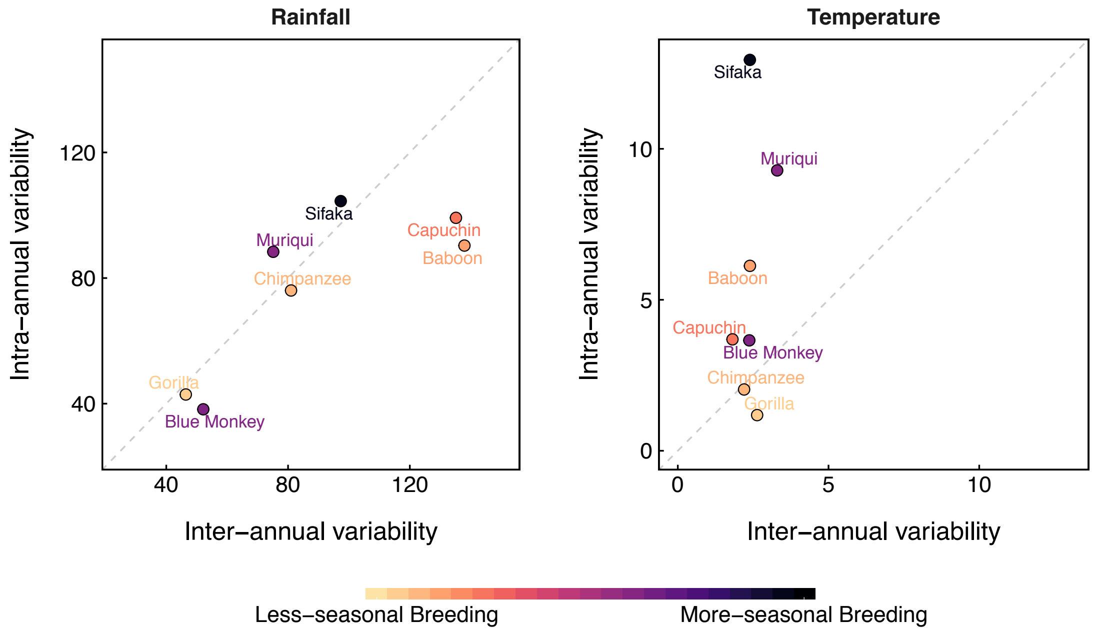

Fig. S13: Intra-annual (i.e., seasonal) and inter-annual climate variability experienced by each study population in relation to degree of breeding seasonality. Let W represent a locally measured climatic variable, either average temperature or total monthly rainfall. Each $W_{m,y}$ is indexed by months $m \in (Jan : Dec)$ and by years $y \in (y_1 : y_n)$, where y_1 is the first year of a study with duration n years. We calculated monthly "climatological" means and coefficients of variation for each month and site: $\mu_m = mean(W_{m,y_1}, \ldots, W_{m,y_n})$ and $CV_m = CV(W_{m,y_1}, \ldots, W_{m,y_n})$. We calculated intra-annual variability as $CV(\mu_m)$. For example, the 37 January rainfall totals for the muriqui site were averaged to calculate μ_{Jan} and this process was repeated for the other 11 months. We then calculated intra-annual variability as $CV(\mu_{Jan}, \ldots, \mu_{Dec})$. We calculated inter-annual variability as $mean(CV_m)$. Again using the muriqui site as an example, we calculated $CV_{Jan}, \ldots, CV_{Dec}$ based on the 37 years of data, and we then calculated inter-annual variability as $mean(CV_{Jan}, \ldots, CV_{Dec})$.

Table S1: Seasonality of births in the seven primate populations. The value of the mean vector (r) indicates how unevenly observations are spread across the annual cycle. When $r = 1$, all births occur on the same day-of-year, and when $r = 0$, the births are evenly distributed across the 12 months. The p values show the results of a Rayleigh test for non-uniformity of circular data. Significant results indicate seasonal reproduction. See also Fig. 4.

Species	**N Births**	**% births in top 3 months**	**% births in bottom 3 months**	**Mean birth day-of-year**	r	p
Verreaux's Sifaka	706	97.5	0.8	23-Jul	0.955	< 0.01
White-faced Capuchin	209	44	13.4	19-May	0.25	< 0.01
Northern Muriqui	376	62.2	4	24-Jul	0.601	< 0.01
Blue Monkey	515	61.9	4.5	12-Feb	0.615	< 0.01
Yellow Baboon	820	32.3	15.5	22-Oct	0.152	< 0.01
Eastern Chimpanzee	198	33.8	16.2	16-Jul	0.107	0.103
Mountain Gorilla	269	41.6	17.5	29-Jun	0.056	0.434